Earth Planets Space, **56**, 103–107, 2004

Crustal deformation associated with the northern Miyagi earthquake detected by RADARSAT-1 and ENVISAT SAR interferometry

Hiroshi Yarai[1], Taku Ozawa[2], Takuya Nishimura[1], Mikio Tobita[1], and Tetsuro Imakiire[1]

[1] *Geography and Crustal Dynamics Research Center, Geographical Survey Institute, Kitasato-1, Tsukuba, Ibaraki 305-0811, Japan*
[2] *Japan Society for the Promotion of Science / Geographical Survey Institute, Kitasato-1, Tsukuba, Ibaraki 305-0811, Japan*

(Received November 22, 2003; Revised February 27, 2004; Accepted February 27, 2004)

We applied synthetic aperture radar (SAR) interferometry to map the deformation field of the northern Miyagi earthquake (M6.4) which occurred on July 26, 2003. RADARSAT-1 and ENVISAT satellite data were processed to show the deformation field associated with the earthquake. This is the first observation of the crustal deformation associated with an earthquake detected by ENVISAT SAR interferometry. The 2.5-dimensional displacement near the epicenter was revealed by the combination of RADARSAT-1 and ENVISAT interferograms. The 2.5-D displacement vectors are consistent with the fault model proposed by Nishimura *et al*. (2003). The InSAR displacement fields show that the boundary of the uplifted and subsided areas is located not along the Asahiyama flexure but 3–4 km east of the flexure. Therefore, the source fault of the earthquake may have little relation to the Asahiyama flexure.

Key words: Crustal deformation, northern Miyagi earthquake, InSAR, RADARSAT, ENVISAT, 2.5D displacement.

1. Introduction

On July 26, 2003, a shallow earthquake (M6.4) occurred in northern Miyagi prefecture, northeastern Japan. The M6.4 earthquake was accompanied by the M5.6 foreshock and the largest M5.5 aftershock on the same day. Coseismic displacement was observed by the Japanese nationwide GPS network (GEONET) maintained by the Geographical Survey Institute (GSI) (Fig. 1). In addition, leveling and campaign GPS observations, carried out by the GSI in Miyagi prefecture just after the earthquake, clearly revealed the coseismic deformation.

These geodetic data indicate that the displacement is limited to an area near the epicenter. The GEONET stations are spaced about 20 km apart, and the leveling benchmarks are installed at about 2 km intervals along national highways. Therefore, geodetic observation stations are too sparse to clarify the deformation field of M6-class earthquakes. We applied the SAR interferometry (InSAR) technique to study the deformation field around the epicentral area in detail.

2. Coseismic Deformation Determined by SAR Interferometry

2.1 SAR interferometry

Before and after the northern Miyagi earthquake, the epicentral region was imaged by the Canadian RADARSAT-1 and the European ENVISAT satellites. The RADARSAT-1 and ENVISAT data could be analyzed by SAR interferometry to map the crustal deformation associated with the earthquake. We used the digital elevation model of 50 m grid developed by the GSI to remove topographic fringes by the two-pass approach (Massonnet *et al*., 1993). We applied adaptive spectral filtering (Goldstein and Werner, 1998) to reduce noise in the interferograms.

2.2 RADARSAT-1 interferogram

The RADARSAT-1 satellite has a C-band SAR whose wavelength is 5.7 cm and polarization is HH. The RADARSAT-1 has various imaging modes with different incidence angle, resolution, and swath width. We used Fine mode data (pixel spacing is about 10 m, swath width is 50 km) in this study. We analyzed F5 mode (incidence angle is 43°) data to generate an interferogram. The RADARSAT-1 data were obtained from descending orbits on June 13 and July 31, 2003.

The interferogram had good coherence in and around populated areas and flat areas (Fig. 2). The phase change that is related to crustal deformation is observed near the epicenter. An enlarged interferogram near the epicenter is shown in Fig. 3(a). Each fringe of the RADARSAT-1 interferogram represents the displacement of 2.85 cm in the line of sight (LOS) to the satellite. The unit vector of the LOS displacement is (−0.719, 0.115, −0.685) in the coordinate set (east, north, up).

The RADARSAT-1 interferogram shows that the range between the surface and the satellite decreases approaching the epicentral area. The largest displacement in the RADARSAT-1 interferogram is observed near the Yamoto GEONET station (Fig. 3(a)). The Yamoto station recorded the largest displacement of the earthquake among all GEONET stations around the epicentral region. The displacement observed by the GPS at the Yamoto station is −16 cm in the RADARSAT-1 LOS direction. It is consistent with the RADARSAT-1 LOS displacement at the Yamoto station,

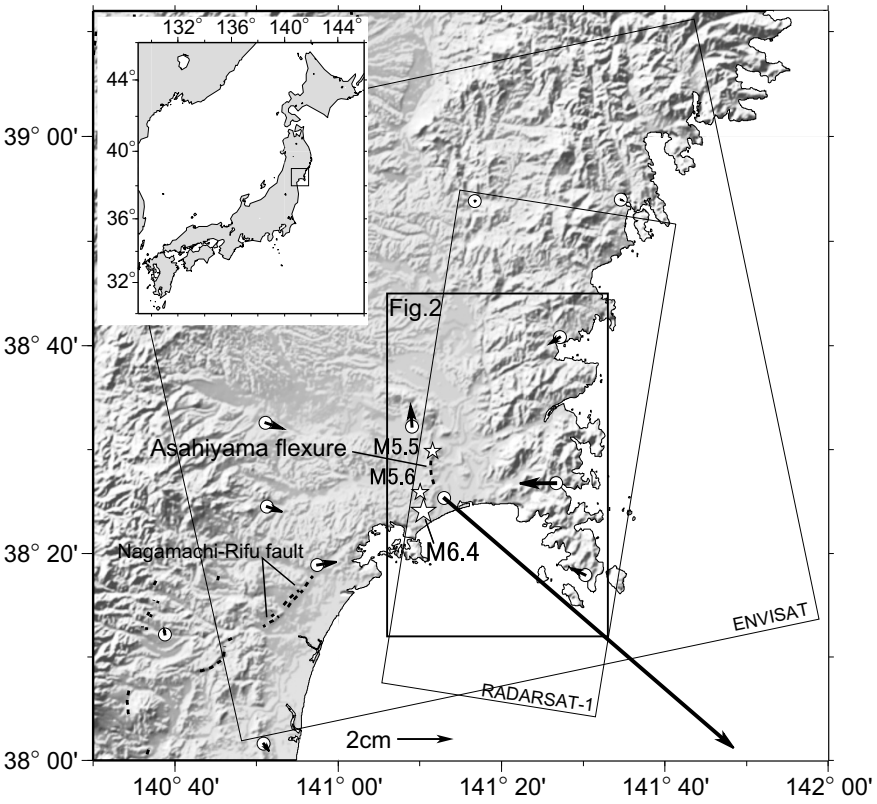

Fig. 1. Shaded-relief topographic map showing geodetic stations and epicenters of earthquakes. Black arrows indicate coseismic horizontal displacement associated with the M6.4 northern Miyagi earthquake at the continuous GPS observation stations with respect to station 970797 (37.9814°E, 140.649°N). Stars with M6.4, M5.6 and M5.5 indicate epicenters of the main shock, the largest foreshock, and the largest aftershock on July 26, 2003, respectively. Open circles indicate locations of the GPS stations. The thick dotted lines indicate surface traces of the Quaternary faults (Active Fault Research Group, 1991). Thin rectangles show the area of the SAR images. The middle box indicates the area covered by Fig. 2.

which is −17 cm. The displacements at other GPS stations are less than 1 cm in the RADARSAT-1 LOS directions. This feature of the GPS observation results is consistent with the RADARSAT-1 interferogram, which shows that coseismic deformation is limited near the epicenter.

Strictly, the fringe shows the total deformation due to the foreshock (M5.6), main shock (M6.4) and largest aftershock (M5.5). However, the deformations near the epicenter of the main shock should be far larger than those of other earthquakes.

2.3 ENVISAT interferogram

The ENVISAT satellite is the newest SAR satellite, which was launched by the European Space Agency in February 2002. The radar operates in the C-band (5.6 cm wavelength). ENVISAT also has various imaging modes with different incidence angle, resolution, and swath width. In addition, the satellite has multi-polarization modes. We used ASAR Image Mode data (pixel spacing is about 30 m, swath width is 100 km). The mode of the generated ENVISAT data is the IS2 mode (incidence angel is 22.8° at the scene center) with VV polarization, which is the ERS-like mode. The ENVISAT data were obtained from ascending orbits on June 27 and August 1, 2003.

Figure 3(b) shows the ENVISAT interferogram, enlarged near the epicenter. Each fringe of the ENVISAT interferogram represents the LOS displacement of 2.8 cm. The LOS unit vector of the ENVISAT interferogram is (0.376, 0.093, −0.922) in the coordinate set (east, north, up). The ENVISAT interferogram clearly shows the coseismic deformation of the earthquake. This is the first observation of the crustal deformation associated with an earthquake detected by ENVISAT SAR interferometry. This suggests that ENVISAT SAR data are useful for detecting crustal deformation by InSAR.

The ENVISAT interferogram shows that the range between the surface and the satellite decreases near the epicenter. The displacement observed by the GPS at the Yamoto GEONET station is −5 cm in the ENVISAT LOS direction. The ENVISAT LOS displacement at the Yamoto station is −3 cm. The ENVISAT result, as well as the RADARSAT-1 result, is almost consistent with the GPS results.

3. 2.5-D Surface Deformation

Two- or three-dimensional InSAR imaging of the displacement is possible by combining measurements from several observation directions (Massonnet *et al.*, 1995, 1996; Fialko *et al.*, 2001). From ascending and descending InSAR images, two distinct LOS vectors are computed. The two vectors lie on one plane, called 'the LOS plane' (Fujiwara *et al.*, 2000). The combination of the ascending and descending InSAR images describes the two-dimensional displacement parallel to the LOS plane at all pixels in the InSAR image. The two-dimensional spatial distribution of the two-dimensional displacement is called the '2.5-D surface deformation map' (Fujiwara *et al.*, 2000).

The 2.5-D surface deformation was calculated from

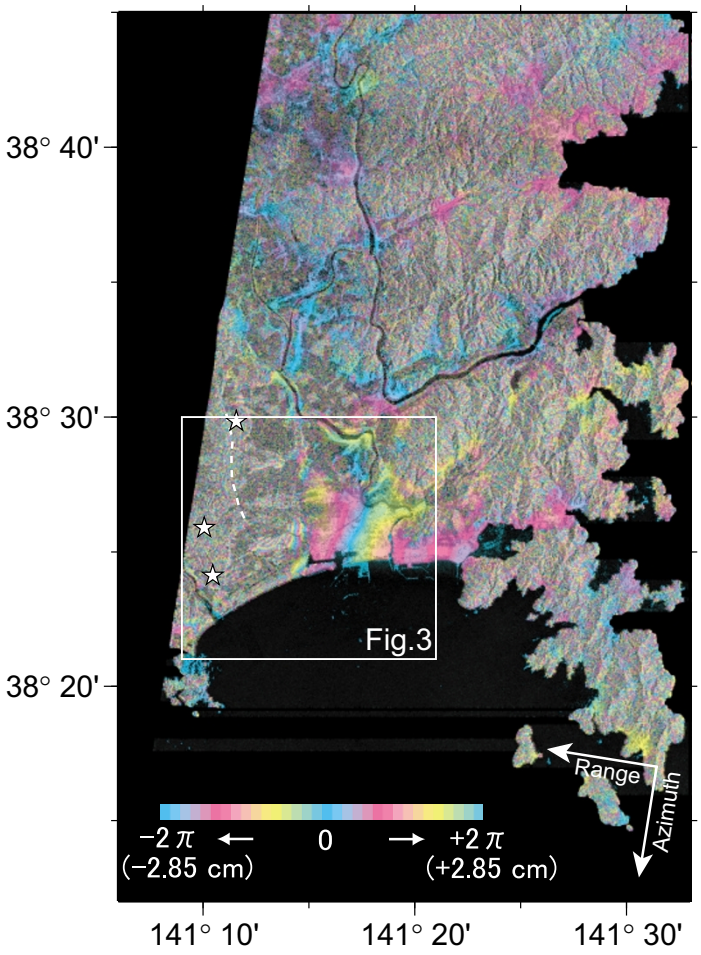

Fig. 2. The RADARSAT-1 interferogram around the epicentral region of the northern Miyagi earthquake. Good coherence can only be obtained in and around populated areas and flat areas. Coherence is poor in rice fields and hills covered by vegetation. The stars indicate epicenters of the main shock, the largest foreshock, and the largest aftershock on July 26, 2003, respectively. The white broken lines indicate the Asahiyama flexure. The white arrows show azimuth and range direction. The area where local surface deformation can be seen in Fig. 3 is indicated by the box.

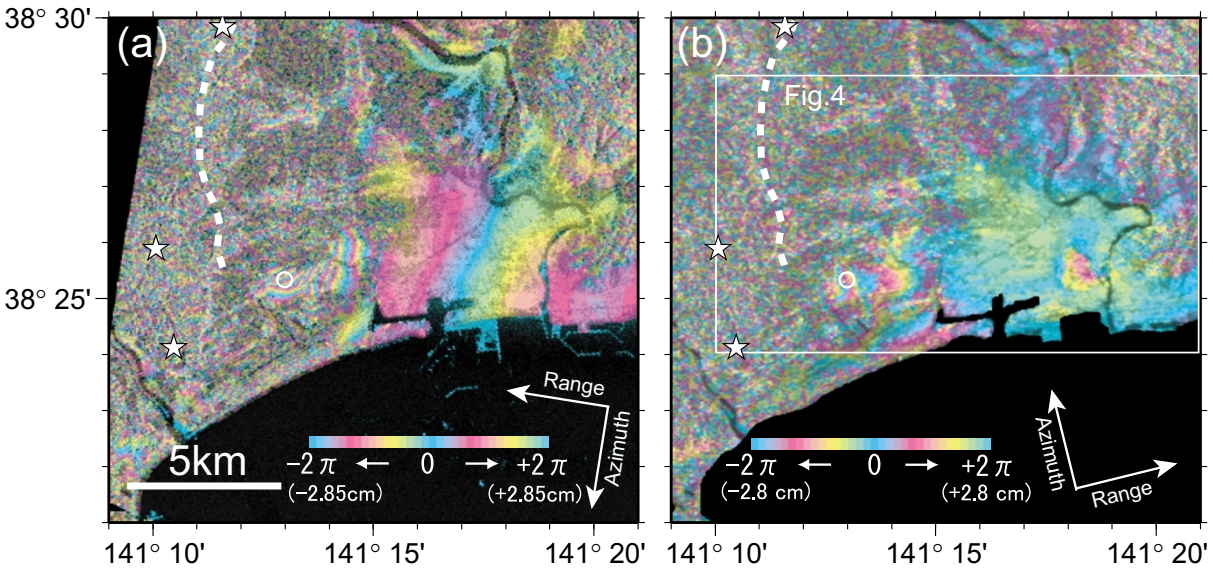

Fig. 3. The enlarged interferograms show the crustal deformation near the epicenter. The white circles indicate the location of the Yamoto GEONET station. The white broken line indicates the Asahiyama flexure (Ishii *et al*., 1982). (a) The RADARSAT-1 interferogram shows the crustal deformation map in which each fringe represents the displacement of 2.85 cm in the line of sight (LOS) to the satellite. The unit vector of the LOS displacement is (−0.719, 0.115, −0.685) in the coordinate set (east, north, up). The RADARSAT-1 data were obtained from descending orbits on June 13 and July 31, 2003. (b) The ENVISAT interferogram shows crustal deformation map in which each fringe represents the LOS displacement of 2.8 cm. The LOS unit vector is (0.376, 0.093, −0.922) in the coordinate set (east, north, up). The ENVISAT data were obtained from ascending orbits on June 27 and August 1, 2003. The small box indicates the area covered by Fig. 4.

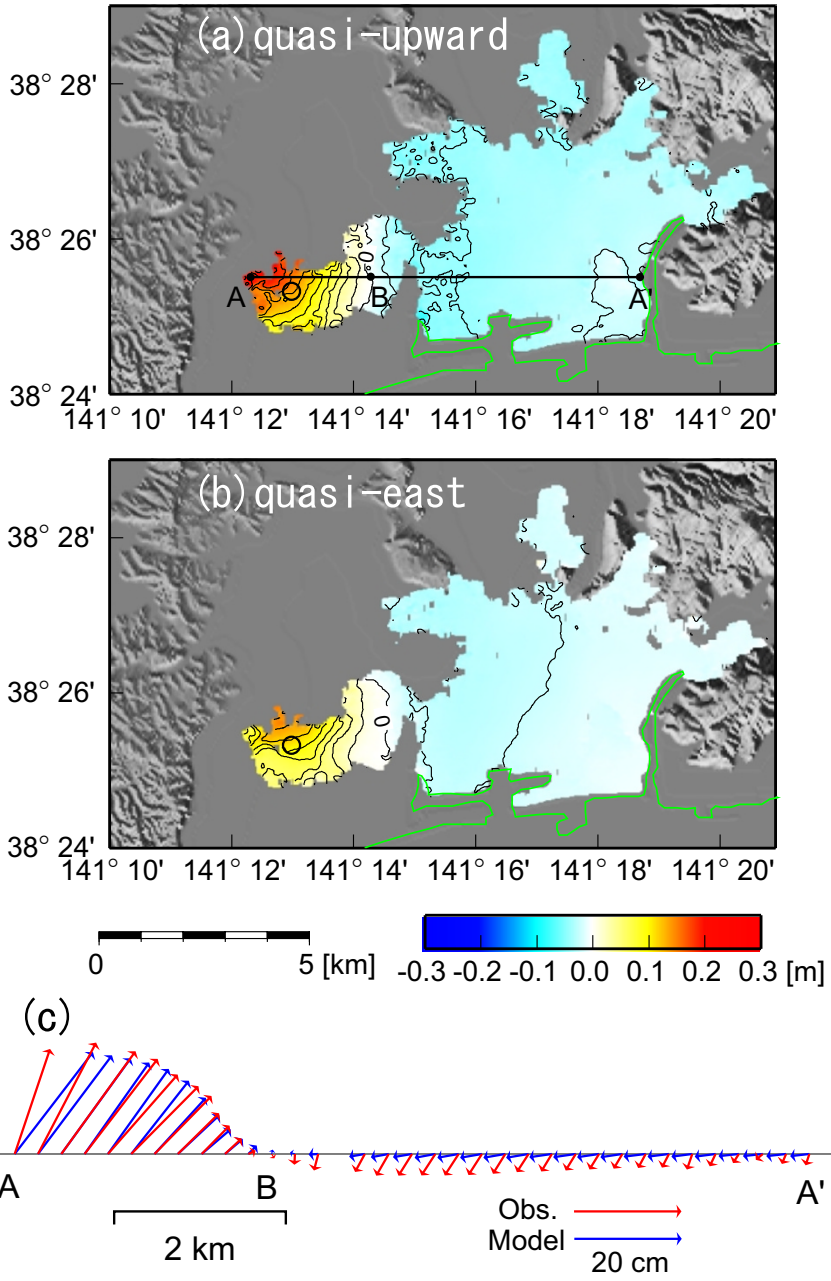

Fig. 4. 2.5-dimensional displacement synthesized from a combination of the RADARSAT-1 and ENVISAT interferograms. Displacement in (a) quasi-upward direction and (b) quasi-eastward direction. Contours indicate movement at intervals of 2 cm. Gray shaded areas are decorrelated because the ground was covered by vegetation. The open circles indicate the location of the Yamoto GEONET station. Yellow arrows indicate the trace of the Asahiyama flexure. (c) Two-dimensional displacement vectors along the line A-A′ shown in (a). Red arrows are synthesized using InSAR and blue arrows are derived from the fault model of Nishimura *et al.* (2003).

the RADARSAT-1 image (descending, Fig. 3(a)) and the ENVISAT image (ascending, Fig. 3(b)). The displacement vector was divided into quasi-upward (elevation angle is 83.2° and it points south-up along the LOS plane) and quasi-eastward (azimuth of the LOS plane is N87.4°W) components (Figs. 4(a), 4(b)). Figure 4(c) shows the 2-D displacement vectors along an east-west line (A-A′).

4. Results and Discussion

The 2.5-D deformation was calculated from the InSAR results (Figs. 4(a), 4(b)). The calculated 2.5-D deformation vectors show that the western part (AB) has been thrust over the eastern part (BA′) (Fig. 4(c)). The InSAR vectors suggest that the western part of the source fault, dipping west, is thrust over the eastern part. Nishimura *et al.* (2003) estimated the rectangular fault model using inversion of geodetic data. Although they did not use the ENVISAT SAR data to construct their model, the 2.5-D displacement vectors (red arrows) are roughly consistent with the predicted displacement vectors (blue arrows) derived from Nishimura *et al.*'s fault model. However, we can point out that there is a discrepancy in the vector direction between our results and the model prediction in Fig. 4(c). Observed subsidence at the eastern part, particularly near B, is underestimated by their model. This implies that the southern end of the source fault may be more south than that of Segment 1 of Nishimura *et*

al.'s model.

The Asahiyama flexure is located in the epicentral region (Figs. 3(a) and 3(b)). The flexure has a north-south strike and the altitude west of the flexure is higher than that east of the flexure. This feature is similar to the coseismic deformation pattern, because the western part was thrust over the eastern part and the boundary between the uplifted and the subsided areas has a north-south strike. Just after the earthquake, it was considered that the Asahiyama flexure was reactivated by the earthquake. The elastic theory of surface displacements due to buried faults (e.g., Okada, 1985) suggests that the boundary of the uplifted and subsided areas approximately marks an extension of the source fault to the surface. If the northern Miyagi earthquake ruptured the fault which forms the Asahiyama flexure, the boundary will be consistent with the trace of the flexure. However, this boundary for the earthquake is located not along the Asahiyama flexure but 3–4 km east of the flexure (Figs. 4(a) and 4(b)). Therefore, the northern Miyagi earthquake did not rupture the fault forming the Asahiyama flexure. We will be able to clarify the relationship between the Asahiyama flexure and the northern Miyagi earthquake on the basis of the crustal deformation field close to the epicentral area where the largest displacement is expected.

We could not clarify the coseismic deformation near the epicenter, because there are mountains and rice fields in and around the epicentral area. C-band microwaves are scattered at the canopy and the surface of grass, whose surface condition changes easily. Therefore, repeat-pass correlation at the C-band becomes poor in vegetated areas (Rosen *et al.*, 1996). In contrast to the C-band, longer wavelength bands such as the L-band are far more robust for repeat-pass interferometry in vegetated areas because microwaves of longer wavelength more easily penetrates the canopy and scatters off trunks and branches (Rosen *et al.*, 1996). Most previous InSAR researchers of crustal deformation in Japanese islands have used SAR data acquired by the Japanese JERS-1 (e.g., Ozawa *et al.*, 1997; Fujiwara *et al.*, 1998), which has the L-band SAR, because most areas other than populated areas are covered by vegetation. However, there are no active L-band SAR satellites in orbit now. The Advanced Land Observation Satellite (ALOS), which is scheduled to be launched by the Japan Aerospace Exploration Agency (JAXA) in 2004, has an L-band SAR. The ALOS SAR will be useful for detecting crustal deformation in vegetated areas, such as mountain areas of Japan.

5. Summary

We applied InSAR measurements using RADARSAT-1 and ENVISAT data to the northern Miyagi earthquake. The generated interferograms yielded maps of the coseismic deformation around the epicentral area. These interferograms are consistent with the GPS measurement results. The ENVISAT interferogram shows that the ENVISAT SAR data are useful for detecting crustal deformation by InSAR.

The 2.5-D displacement was calculated using a combination of RADARSAT-1 and ENVISAT interferograms. The 2.5-D displacement vectors are consistent with the simulated vectors derived from the fault model by Nishimura *et al.* (2003).

The InSAR displacement fields show that the boundary of the uplifted and subsided areas is located not along the Asahiyama flexure but 3–4 km east of the flexure. Therefore, the source fault of the earthquake may be unrelated to the formation in the Asahiyama flexure. We could not clarify their relationship due to the poor coherence in the vegetation-covered epicentral area. If we could use L-band SAR data, we would be able to clarify the relationship on the basis of the crustal deformation near the epicenter.

Acknowledgments. We thank members of the Research Planning Div. and Satellite Geodesy Div. of the Geographical Survey Institute for providing the geodetic data and the information on the epicentral area. We are grateful to Naoyuki Fujii and the anonymous reviewer for useful review and suggestions. The hypocentral data were provided by the Japan Meteorological Agency in cooperation with the Ministry of Education, Culture, Sports, Science and Technology. RADARSAT-1 data were received by the Canada Centre for Remote Sensing. Original ENVISAT data were distributed by Eurimage. We used Generic Mapping Tools (Wessel and Smith, 1998) to plot most figures.

References

Active Fault Research Group, Active Fault in Japan: sheet maps and inventories (Revised edition), 437 pp., University of Tokyo Press, Tokyo, 1991 (in Japanese).

Fialko, Y., M. Simons, and D. Agnew, The complete (3-D) surface displacement field in the epicentral area of the 1999 Mw7.1 Hector Mine earthquake, California, from space geodetic observations, *Geophy. Res. Let.*, **28**, 3063–3066, 2001.

Fujiwara, S., P. Rosen, M. Tobita, and M. Murakami, Crustal deformation measurements using repeat-pass JERS 1 synthetic aperture radar interferometry near the Izu Penisula, Japan, *J. Geophys. Res.*, **103**, 2411–2426, 1998.

Fujiwara, S., T. Nishimura, M. Murakami, H. Nakagawa, and M. Tobita, 2.5-D surface deformation of M6.1 earthquake near Mt Iwate detected by SAR interferometry, *Geophy. Res. Let.*, **27**, 2049–2052, 2000.

Goldstein, R. M. and C. L. Werner, Radar interferogram filtering for geophysical applications, *Geophy. Res. Let.*, **25**, 4035–4038, 1998.

Ishii, T., Y. Yanagisawa, S. Yamaguchi, A. Sangawa, and K. Matsuno, Geology of the Matsushima district, 121 pp., Geological Survey of Japan, 1982 (in Japanese with English abstract).

Massonnet, D., K. L. Rossi, C. Carmona, F. Adragna, G. Peltzer, K. Fiegl, and T. Rabaute, The displacement field of the Landers earthquake mapped by radar interferometry, *Nature,* **364**, 138–142, 1993.

Massonnet, D., P. Briole, and A. Arnaud, Deflation of Mount Etna monitored by spaceborne radar interferometry, *Nature,* **375**, 567–570, 1995.

Massonnet, D., K. Feigl, H. Vadon, and M. Rossi, Coseismic deformation field of the M = 6.7 Northridge, California earthquake of January 17, 1994 recorded by two radar satellites using interferometry, *Geophy. Res. Let.*, **23**, 969–972, 1996.

Nishimura, T., T. Imakiire, H. Yarai, T. Ozawa, M. Murakami, and M. Kaidzu, A preliminary fault model of the 2003 July 26, M6.4 northern Miyagi earthquake, northeastern Japan, estimated from joint inversion of GPS, leveling, and InSAR data, *Earth Planets Space,* **55**, 751–757, 2003.

Okada, Y., Surface deformation due to shear and tensile faults in a half-space, *Bull. Seismol. Soc. Am.*, **75**, 1135–1154, 1985.

Ozawa, S., M. Murakami, S. Fujiwara, and M. Tobita, Synthetic aperture radar interferogram of the 1995 Kobe earthquake and its geodetic inversion, *Geophy. Res. Let.*, **24**, 2327–2330, 1997.

Rosen, P. A., S. Hensley, H. A. Zebker, F. H. Webb, and E. J. Fielding, Surface deformation and coherence measurements of Kilauea Volcano, Hawaii, from SIR-C radar interfeormetry, *J. Geophys. Res.*, **101**, 23109–23125, 1996.

Wessel, P and W. H. F. Smith, New improved version of generic mapping tools released, *Eos Trans. AGU,* **79**(47), 579, 1998.

H. Yarai (e-mail: yarai@gsi.go.jp), T. Ozawa, T. Nishimura, M. Tobita, and T. Imakiire